

Time-dependent single electron tunneling through a shuttling nanoisland

G. Cohen, V. Fleurov, and K. Kikoin

Raymond and Beverly Sackler Faculty of Exact Sciences, School of Physics and Astronomy, Tel-Aviv University, Tel-Aviv 69978, Israel

(Received 11 March 2009; revised manuscript received 5 May 2009; published 11 June 2009)

We offer a general approach to the calculation of single electron tunneling spectra and conductance of a shuttle oscillating between two half-metallic leads with fully spin-polarized carriers. In this case the spin-flip processes are completely suppressed and the problem may be solved by means of canonical transformation, where the adiabatic component of the tunnel transparency is found exactly, whereas the nonadiabatic corrections can be taken into account perturbatively. Time-dependent corrections to the tunnel conductance of moving shuttle become noticeable at finite bias in the vicinity of the even/odd occupation boundary at the Coulomb diamond diagram.

DOI: [10.1103/PhysRevB.79.245307](https://doi.org/10.1103/PhysRevB.79.245307)

PACS number(s): 73.21.La, 73.23.Hk

I. INTRODUCTION

Single electron tunneling (SET) is a salient feature of quantum transport in nanostructures. The SET phenomenon is observed in various systems, e.g., quantum dots (QDs) in a tunnel contact with metallic electrodes,^{1,2} molecular bridges between the edges of broken metallic wires,^{3–5} atoms and molecules absorbed on metallic surfaces in a contact with the tip of tunnel microscope,^{6,7} etc. The study of electron tunneling through the nano-object with time-dependent characteristics is one of the most challenging problems in this field.

There are several sources of time dependence, which may be realized in practical devices. The simplest one is the time-dependent gate voltage $v_g(t)$ applied to the dot. It is well known^{8–10} that this time dependence may be converted into the time dependence of tunnel matrix element. Another possibility is the nanoelectromechanical shuttling (NEMS),¹¹ where the nanosize island suspended on a pivot¹² or attached to a string¹³ oscillates between the leads under the action of an electromechanical force. In the case of molecular bridges, the vibration eigenmodes may be the source of the periodical oscillations of tunneling parameters.^{5,14}

Usually the tunneling between metallic leads and such a nano-object is accompanied by many-particle Kondo screening effect^{15,16} resulting in a specific type of zero-bias anomaly (ZBA) in the tunnel conductance. Modification of Kondo regime because of periodically modulated in time tunneling rate due to the center-of-mass oscillations was studied recently in several papers. If the oscillations are the eigenmodes of a nano-object (molecule), then the Kondo peak (zero-bias anomaly in the tunnel conductance) may transform into a dip due to the destructive interference with the vibrational mode.¹⁴ In the case of adiabatic motion induced by electromechanical forces (NEMS) (Ref. 11), the Kondo temperature follows the periodical evolution of the dot position and increases eventually due to the effective reduction in the average distance between the dot and the leads,¹⁷ which is determined by the mean-square displacement of the dot (in an analogy with the Debye-Waller effect in the scattering intensity). A nonadiabatic enhancement of Kondo tunneling through such moving nano-object at a finite source-drain bias has been studied recently.¹⁸

In the present paper we consider adiabatic and nonadiabatic time-dependent effects in conventional cotunneling be-

tween metallic leads due to a periodic modulation of the lead-dot tunneling rate. To suppress the many-particle Kondo screening effects, one should consider the leads with magnetically polarized electrons. Tunneling between the ferromagnetically ordered leads was discussed in the context of Kondo effect.^{19–25} We are interested in the situation, where the spin-flip cotunneling is completely suppressed at small lead-dot bias and low temperatures. Such tunneling regime may be realized in half-metallic ferromagnets, where the Fermi surface is formed only by the majority-spin electrons, whereas the spectrum of the minority-spin carriers is gapped. The electronic and magnetic properties of such metallic compounds are reviewed in Ref. 26. From the point of view of existing devices, where the leads are formed by two-dimensional (2D) electrons in degenerate semiconductors, the relevant material for our studies is a dilute magnetic semiconductor (Ga,Mn)As.²⁷ The indirect magnetic exchange between Mn impurity ions is responsible for the long-range ferromagnetic order in this material. This exchange is mediated by spin-polarized carriers near the top of the valence band. The tunnel current in the half-metallic regime arises due to the minority-spin hole cotunneling.

We will show that in the absence of Kondo effect the problem of tunneling through a moving nanoisland (quantum dot) may be solved by means of *time-dependent canonical transformation*, which exactly takes into account both adiabatic and nonadiabatic lead-dot tunneling processes diagonal in the lead indices. The nondiagonal source-drain cotunneling may be treated by the canonical transformation method only perturbatively, but the adiabatic and nonadiabatic contributions into tunnel conductance may be sorted out also in this case. It will be shown that the time-dependent contribution into current-voltage characteristics of moving nano-object is significant near the boundaries of Coulomb diamonds.

II. MODEL

We choose for the realization of ac-driven tunnel conductivity the simplest model of a nano-object, which is widely used in the studies of SET. The nano-object is represented in this model by the quantum well with a resonance level ε_d (see Fig. 1, upper panel). The SET regime arises due to the

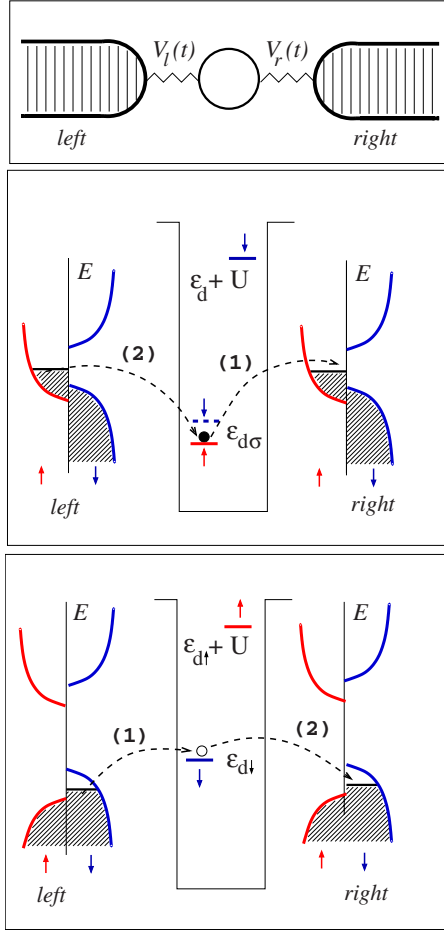


FIG. 1. (Color online) Upper panel: model of a quantum dot in a time-dependent contact with leads. Middle and lower panels: density of electron states in the leads and occupied and empty states in the dot for $N=1$; mechanisms of spin-polarized electron cotunneling (middle panel) and hole cotunneling (lower panel) are indicated by arrows. Figures in parentheses point out the sequence of electron tunneling acts in the cotunneling processes.

Coulomb blockade effect: addition energy for the second electron in a singly occupied dot is $\varepsilon_d + U \gg \Gamma_j$, where Γ_j is the tunneling rate to the left ($j=l$) and right ($j=r$) leads, and U is the capacitive energy of the dot. To separate the time-dependent SET from the Kondo ZBA, we consider tunneling between spin-polarized leads, where spin-flip processes are inelastic, because the continuum of electron-hole pairs with the opposite spins in the leads responsible for the Kondo effect is gapped. Two types of spin-polarized (magnetically ordered) metallic leads are presented schematically in Fig. 1. In the middle panel the leads are formed by “half-metallic ferromagnets”²⁶ with gapped spectrum of minority-spin carriers. In the lower panel characteristic for the p -type degenerate dilute magnetic semiconductors,²⁷ the carriers are the minority-spin holes.

Virtual tunneling results in a shift of level positions in QD. This renormalization (“Friedel shift”) is also spin dependent. As a result the spin polarization of QD adjusts to that of the ferromagnetic lead (see calculations below). All Kondo processes are quenched in this regime.

The Anderson Hamiltonian modeling SET has the form

$$H = H_d + H_b + H_{\text{tun}}, \quad (2.1)$$

where the terms

$$H_d = \sum_{\Lambda} E_{\Lambda} |\Lambda\rangle \langle \Lambda|, \quad H_b = \sum_{j=l,r} \sum_{k\sigma} \epsilon_{jk\sigma} a_{jk\sigma}^{\dagger} a_{jk\sigma} \quad (2.2)$$

describe the electron states in the isolated dot and two metallic (semiconductor) leads, respectively. We write H_d in terms of its eigenstates $|\Lambda\rangle$ (Hubbard representation). This trick allows one to take all intradot interactions into account exactly even when the contact with the leads is switched on. The tunneling Hamiltonian

$$H_{\text{tun}} = \sum_{jk\sigma} (V_{jk} d_{\sigma}^{\dagger} a_{jk\sigma} + \text{H.c.})$$

may be rewritten in the Hubbard representation by expanding the creation operator d_{σ}^{\dagger} in terms of the configuration change operators $X^{\Lambda\lambda} = |\Lambda\rangle \langle \lambda|$ which connects the states in adjacent charge sectors with N and $N-1$ electrons in the dot. We confine ourselves with the simplest case, where only three charge sectors $N=0,1,2$ are involved in SET Hamiltonian. Then Hamiltonian (2.1) acquires the following form:

$$H = \varepsilon_d \sum_{\sigma} X^{\sigma\sigma} + E_2 X^{22} + \sum_{jk\sigma} \epsilon_{jk\sigma} a_{jk\sigma}^{\dagger} a_{jk\sigma} + \sum_{jk\sigma} [V_{jk} a_{jk\sigma}^{\dagger} (X^{0\sigma} + \sigma X^{\bar{\sigma}2}) + \text{H.c.}], \quad (2.3)$$

Here the quantum numbers $\Lambda, \lambda=0, \sigma, 2$ correspond to empty, singly, and doubly occupied states of QD, respectively, and $E_2 = 2\varepsilon_d + U$ is the energy of doubly occupied QD. The last term in this Hamiltonian is time dependent.

III. CANONICAL TRANSFORMATION OF ANDERSON HAMILTONIAN

Our program is to exclude the tunneling term from Hamiltonian (2.3) by means of the canonical transformation

$$\tilde{H} = e^S H e^{-S}, \quad (3.1)$$

then derive the tunnel current operator in the new basis and calculate the tunnel conductance. It was shown in Ref. 28 that this transformation may be performed exactly in the absence of Coulomb correlation, provided the energy level ε_d falls into the energy gap and remains there after renormalization (Friedel shift). It will be shown below that the matrix S still may be found exactly in the presence of Coulomb blockade under the same condition of discreteness of renormalized d -level, provided the spin-flip processes are quenched. As may be perceived from Fig. 1, this condition is realized for the majority-spin electrons in the case of half-metallic ferromagnet and for the minority-spin holes in the case of p -type dilute magnetic semiconductor.

As usual, the canonical transformation is made by means of the Baker-Hausdorff expansion

$$e^S H e^{-S} = \sum_{n=0}^{\infty} \frac{1}{n!} [S, [S, \dots [S, H] \dots]]. \quad (3.2)$$

In the noninteracting case, the second quantization operators in S and H possess Fermi-like commutation relations, the Hamiltonian H is a quadratic form, and the tunnel operator conserves spin, so the series in the right-hand side (r.h.s.) of Eq. (3.2) may be summed exactly.²⁸ The Coulomb blockade separates the Hilbert space for the dot electron operators into the charge sectors divided by the energy gaps. As a result these operators lose the simple Fermi statistics.

We are interested in the strong Coulomb blockade case and start with the simplest case, when the ground state of the dot corresponds to $N=1$ in the limit of $U \gg |\epsilon_d - \epsilon_F|$, so that the doubly occupied states are completely suppressed. Then only the states $\Lambda = \sigma, 0$ are retained in Hamiltonian (2.3). In particular, the anticommutation relation for the Hubbard operators mixing the adjacent sectors $N=0, 1$ has the form

$$[X^{\sigma 0}, X^{0 \sigma'}]_+ = X^{\sigma \sigma'} + X^{00} \delta_{\sigma \sigma'}, \quad (3.3)$$

which follows from the obvious multiplication rule $X^{\Lambda_1 \Lambda_1} X^{\Lambda_2 \Lambda_2} = \delta_{\Lambda_1 \Lambda_2} X^{\Lambda_1 \Lambda_2}$. Even disregarding the spin-flip processes each commutation operation in expansion (3.2) generates operators $K^\sigma = X^{\sigma \sigma} + X^{00}$. In spite of this, the Baker-Hausdorff series still can be summed exactly, because these operators are idempotent, $K^\sigma K^\sigma = K^\sigma$, like the conventional fermion occupation operators $d_\sigma^\dagger d_\sigma$. This summation will be performed in the following section.

The time-dependent problem is more complicated because in that case the canonical transformation should be applied to the operator

$$\mathcal{L} = -i\hbar \frac{\partial}{\partial t} + H. \quad (3.4)$$

In Sec. III B we will show that the canonical transformation is operational in this case as well, at least in some important special cases.

A. Time-independent transformation

In this section we generalize the canonical transformation proposed for an Anderson model applied to transition-metal impurities in semiconductors.^{28,29} In those calculations the intraimpurity Coulomb interaction was taken into account in the Hartree approximation. Here we take the Coulomb blockade term exactly, when summing series (3.2), at least in the charge sectors $N=0, 1$. The anti-Hermitian operator S is looked for in the form

$$S = \sum_{jk\sigma} (u_{jk\sigma} a_{jk\sigma}^\dagger X^{0\sigma} - u_{jk\sigma}^* X^{\sigma 0} a_{jk\sigma}) = \sum_{\sigma} S_{\sigma}.$$

If the spin-flip processes are neglected, the canonical transformation is made for each spin projection separately. One may apply the transformation to the majority spin in the case of electron tunneling and to the minority spin in the case of hole tunneling in two models introduced above.

One straightforwardly derives the commutation relations

$$[S_{\sigma}, X^{\sigma 0}] = \sum_{jk} u_{jk\sigma} a_{jk\sigma}^\dagger K^{\sigma} \equiv C_{\sigma}^\dagger K^{\sigma},$$

$$[S_{\sigma}, a_{jk\sigma}^\dagger] = -u_{jk\sigma}^* X^{\sigma 0}.$$

To shorten the notations, we introduce the quantities $C_{\sigma}^\dagger = \sum_{jk} u_{jk\sigma} a_{jk\sigma}^\dagger$ and $\gamma_{\sigma}^2 = \sum_{jk} u_{jk\sigma} u_{jk\sigma}^*$. Besides, we omit the lead index j and specify the band state by a single index k characterizing both the lead and the electron wave number. Using these definitions and the above-mentioned idempotency of the operator K_{σ} , we obtain the following expressions for the transformed operators:

$$\tilde{X}^{\sigma 0} = e^{S_{\sigma}} X^{\sigma 0} e^{-S_{\sigma}} = X^{\sigma 0} \cos \gamma_{\sigma} + C_{\sigma}^\dagger K^{\sigma} \gamma_{\sigma}^{-1} \sin \gamma_{\sigma}, \quad (3.5)$$

$$\begin{aligned} \tilde{a}_{k\sigma}^\dagger &= e^{S_{\sigma}} a_{k\sigma}^\dagger e^{-S_{\sigma}} = a_{k\sigma}^\dagger + u_{k\sigma}^* C_{\sigma}^\dagger K^{\sigma} \gamma_{\sigma}^{-2} (\cos \gamma_{\sigma} - 1) \\ &\quad - u_{k\sigma}^* X^{\sigma 0} \gamma_{\sigma}^{-1} \sin \gamma_{\sigma}, \end{aligned} \quad (3.6)$$

and

$$e^{S_{\sigma}} C_{\sigma}^\dagger e^{-S_{\sigma}} = C_{\sigma}^\dagger + C_{\sigma}^\dagger K^{\sigma} (\cos \gamma_{\sigma} - 1) - X^{\sigma 0} \gamma_{\sigma} \sin \gamma_{\sigma}. \quad (3.7)$$

The tunneling term in the transformed Hamiltonian is eliminated, provided

$$u_{k\sigma} = \frac{\gamma_{\sigma} V_k}{(\epsilon_{k\sigma} - E_{d\sigma}) \tan \gamma_{\sigma}} \equiv g_{k\sigma} V_k \quad (3.8)$$

with

$$\tan^2 \gamma_{\sigma} = - \left. \frac{dL_{\sigma}(\epsilon)}{d\epsilon} \right|_{\epsilon=E_{d\sigma}}, \quad (3.9)$$

$$L_{\sigma}(\epsilon) = \sum_k \frac{|V_k|^2}{\epsilon - \epsilon_{k\sigma}}. \quad (3.10)$$

Then the transformed Hamiltonian takes the form

$$\tilde{H}_{\sigma} = E_{d\sigma} X^{\sigma \sigma} + \sum_{kk'} \tilde{\epsilon}_{kk'}^{\sigma} a_{k\sigma}^\dagger a_{k'\sigma}, \quad (3.11)$$

where the renormalized level position is given by the equation

$$E_{d\sigma} = \frac{\epsilon_d + Z_{\sigma} \tan^2 \gamma_{\sigma} - (T_{\sigma} + T_{\sigma}^*) \tan \gamma_{\sigma}}{1 + \tan^2 \gamma_{\sigma}}, \quad (3.12)$$

with $Z_{\sigma} = \gamma_{\sigma}^{-2} \sum_{k\sigma} \epsilon_{k\sigma} u_{k\sigma}^* u_{k\sigma}$ and $T_{\sigma} = \gamma_{\sigma}^{-1} \sum_k (V_k u_{k\sigma}^*)$. Substitution of Eqs. (3.8)–(3.10) into Eq. (3.12) transforms it into the conventional form^{28,29}

$$E_{d\sigma} = \epsilon_d + L_{\sigma}(E_{d\sigma}), \quad (3.13)$$

where the self-energy $L_{\sigma}(E)$ has only real part (Friedel shift), provided the level $E_{d\sigma}$ remains within the gap, which is the case for $\sigma = \uparrow$ in the configuration presented in the middle panel of Fig. 1.

The canonical transformation for the second spin component $\sigma = \downarrow$ should be done more carefully, because the bare level ϵ_d falls into continuum of spin-down states. One should

be cautious with turning to the thermodynamic limit, where the sum in the right-hand side of Eq. (3.10) transforms into the integral and acquires the imaginary part, thus making the Hamiltonian non-Hermitian. The problem can be avoided. The recipe is to keep the spectrum of electrons in the leads discreet when doing the canonical transformation. Then Eq. (3.13) has $\mathcal{N}+1$ solutions ε_i , where \mathcal{N} is the number of states in the valence band $\varepsilon_{k\downarrow}$. Using Eqs. (3.9) and (3.10), the corresponding coefficients γ_i may be found. In accordance with Eq. (3.5), the factor $\cos \gamma_i$ determines the weight of the d component in the hybridized wave function of the dot electron in the state i . One may identify the state $i=m$ producing the maximum value of $\cos \gamma_i$ with the center of future Friedel resonance, which arises in the thermodynamic limit $\mathcal{N} \rightarrow \infty$. In this sense the state $E_{d\downarrow} \equiv \varepsilon_{m\downarrow}$ is formally defined from the equation $\varepsilon_{m\downarrow} = \varepsilon_d + L_{\downarrow}(\varepsilon_{m\downarrow})$. This level is shown by the dashed line in the middle panel of Fig. 1. It corresponds to the bunch of excited states of QD coupled to the leads with $N=1$ and spin oriented antiparallel to that of the magnetized leads.

The spectrum of continuous part of Hamiltonian (3.11) is determined by the expression

$$\tilde{\varepsilon}_{kk'}^{\sigma} = \varepsilon_{k\sigma} \delta_{kk'} + W_{kk'}^{\sigma} \quad (3.14)$$

containing the “scattering” matrix element, which eventually predetermines the tunnel current. The general form of this matrix element is

$$\begin{aligned} W_{kk'}^{\sigma} = & \frac{u_{k\sigma} u_{k'\sigma}^*}{\gamma_{\sigma}^2} K^{\sigma} \left[(2\varepsilon_d - \varepsilon_{k\sigma} - \varepsilon_{k'\sigma})(1 - \cos \gamma_{\sigma}) \right. \\ & \left. - \frac{T_{\sigma} + T_{\sigma}^*}{2} \frac{2 \cos^3 \gamma_{\sigma} - 3 \cos^2 \gamma_{\sigma} + 1}{\cos \gamma_{\sigma} \sin \gamma_{\sigma}} \right] \\ & + K^{\sigma} (V_k u_{k'\sigma}^* + u_{k\sigma} V_{k'}^*) \frac{\sin \gamma_{\sigma}}{\gamma_{\sigma}}. \end{aligned} \quad (3.15)$$

Using Eqs. (3.8) and (3.12) we get

$$T_{\sigma} = T_{\sigma}^* = -\frac{1}{\tan \gamma_{\sigma}} L_{\sigma}(E_{d\sigma})$$

and after some algebraic manipulations the scattering matrix element is eventually transformed into a quite compact expression,

$$\bar{W}_{kk'}^{\sigma} = V_k V_{k'}^* K^{\sigma} \left[\left(\frac{1}{\Delta_{k\sigma}} + \frac{1}{\Delta_{k'\sigma}} \right) R(\gamma_{\sigma}) + \frac{L_{\sigma}(E_{d\sigma})}{\Delta_{k\sigma} \Delta_{k'\sigma}} R^2(\gamma_{\sigma}) \right], \quad (3.16)$$

where

$$R(\gamma_{\sigma}) = \frac{\sqrt{1 + \tan^2 \gamma_{\sigma}} - 1}{\tan^2 \gamma_{\sigma}} \quad (3.17)$$

and $\Delta_{k\sigma} = E_{d\sigma} - \varepsilon_{k\sigma}$. Equation (3.16) holds only in the static case or, as we will see below, for adiabatically slow time variations of the tunneling amplitudes. If we want to study nonadiabatic corrections a more general formula (3.15) should be used.

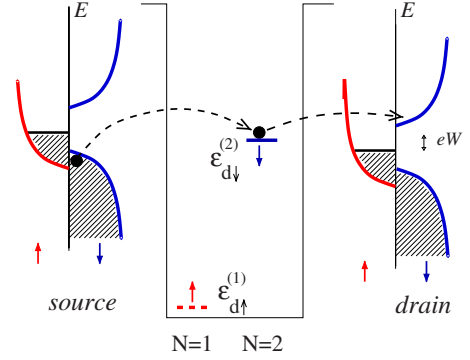


FIG. 2. (Color online) Cotunneling mechanism in the resonance regime for second electron in QD on the boundary of Coulomb window.

Equation (3.16) generalizes the familiar second-order expression for the single electron tunneling amplitude through the QD, which takes into account both the renormalization of the energy level of dot electron (3.13) and the reconstruction of the band continuum (3.6). Far from the resonance tunneling regime (in the center of the Coulomb diamond diagram; see, e.g., the middle panel of Fig. 1), one may neglect the second term in the square bracket of Eq. (3.16), and the tunneling matrix element acquires the simple form $W_{lk,rk'}^{\sigma} = J_{lk,rk'} K^{\sigma} R(\gamma_{\sigma})$, where the first factor is the off-diagonal matrix element of indirect exchange between the leads and the dot due to electron cotunneling and the second and the third factors regulate the occupation of the dot level and the normalization of electron wave functions, respectively. The transparency of QD is, of course, exponentially weak

Now we turn to the resonance regime illustrated by Fig. 2, where the level $\varepsilon_d^{(2)} = \varepsilon_d + U$ driven by the gate voltage v_g approaches the level ε_F from above. The level $\varepsilon_d^{(2)}$ may be occupied only by a spin-down electron. Since it falls into the gap of spin-down density of states in the leads, the canonical transformation introduced above may be performed in a similar way, provided the addition energy for the first electron $\varepsilon^{(1)} \approx \varepsilon_d$ falls deep enough below ε_F and excitations of electrons in this level are suppressed. In this regime $\Lambda, \lambda = \sigma, 2$, and one should use the commutation relations

$$[X^{\sigma 2}, X^{2\sigma'}]_{+} = X^{\sigma\sigma'} + X^{22} \delta_{\sigma\sigma'} \quad (3.18)$$

instead of Eq. (3.3). Correspondingly, one should insert $K^{\sigma} = X^{\sigma\sigma} + X^{22}$ in equations

$$\tilde{X}^{2\bar{\sigma}} = \sigma X^{2\bar{\sigma}} \cos \gamma_{\sigma} + C_{\sigma}^{\dagger} K^{\sigma} \gamma_{\sigma}^{-1} \sin \gamma_{\sigma}, \quad (3.19)$$

$$\tilde{a}_{\sigma}^{\dagger} = a_{k\sigma}^{\dagger} + u_{k\sigma}^* C_{\sigma}^{\dagger} K^{\sigma} \gamma_{\sigma}^{-2} (\cos \gamma_{\sigma} - 1) - u_{k\sigma}^* \sigma X^{2\bar{\sigma}} \gamma_{\sigma}^{-1} \sin \gamma_{\sigma} \quad (3.20)$$

for the transformed creation operators.

Then the transformed Hamiltonian for spin-down electrons has the form

$$\tilde{H}_\downarrow = E_{d\downarrow} X^{\downarrow\downarrow} + \sum_{kk'} \tilde{\epsilon}_{kk'}^\sigma a_{k\downarrow}^\dagger a_{k'\downarrow}, \quad (3.21)$$

where $E_{d\downarrow}$ and $\tilde{\epsilon}_{kk'}^\sigma$ are given by the same equations (3.13) and (3.14) as in the previous case, but with the energy $\epsilon_d^{(2)}$ substituting for ϵ_d and the correlation function K^σ taken from Eq. (3.18). It should be stressed that the tunneling through the QD is impossible at zero source-drain bias because of the spin blockade in spin-polarized electrodes. Only spin-up carriers exist around Fermi level, and these electrons may be injected into the QD only when accompanied by the spin-flip excitations given by the operators $X^{\downarrow\uparrow}$ in the intermediate state with $N=1$ of cotunneling process. These processes are inelastic and exponentially weak ($\sim V^2$ in transparency and $\sim V^4$ in conductance). A more detailed discussion of the spin-dependent tunneling is postponed until Sec. IV A.

B. Time-dependent transformation

As was discussed above experimental conditions may be created when the tunneling matrix element $V_k(t)$ in Hamiltonian (2.3) becomes time dependent. The canonical transformation (3.1), as described in the previous section, cannot be straightforwardly applied. Its generalization is in order.

We start with the time-dependent Schrödinger equation

$$\mathcal{L}\psi = 0 \quad (3.22)$$

[see Eq. (3.4)] and look for the time-dependent transformation matrix $\tilde{S}(t)$, which transforms Eq. (3.22) into

$$\tilde{\mathcal{L}}\tilde{\psi} = 0 \quad (3.23)$$

with transformed operator

$$\tilde{\mathcal{L}}(t) = e^{S(t)} H e^{-S(t)} - i\hbar e^{S(t)} \frac{\partial}{\partial t} e^{-S(t)}$$

for the new wave function $\tilde{\psi} = e^{S(t)} \psi$. The Hamiltonian \tilde{H} satisfying Eq. (3.23) can be written as

$$\tilde{H} = e^S H e^{-S} + i\hbar \int_0^1 d\lambda e^{\lambda S} \dot{S} e^{-\lambda S} \quad (3.24)$$

(see Appendix A).

Hamiltonian (3.24) contains now two terms, of which the first one is just a modification of Hamiltonian (3.1) of the time-independent case. It means that all the equations in Sec. III A hold except for Eq. (3.8), which defines the coefficients $u_{k\sigma}$ of the canonical transformation. These coefficients must be now found anew. There is also the second term in the right-hand side of Eq. (3.24), which is responsible for nonadiabatic effects.

In order to find the canonical transformation parameters $u_{k\sigma}$ we write explicitly the condition

$$\begin{aligned} & u_{k\sigma} \gamma_\sigma^{-1} [(\epsilon_d - Z_\sigma) \sin \gamma_\sigma \cos \gamma_\sigma - (\epsilon_{k\sigma} - Z_\sigma) \sin \gamma_\sigma \\ & + T_\sigma \cos^2 \gamma_\sigma - T_\sigma^* \sin^2 \gamma_\sigma - T_\sigma \cos \gamma_\sigma] \\ & + V_k \cos \gamma_\sigma = -i\hbar \dot{u}_{k\sigma} \frac{\sin \gamma_\sigma}{\gamma_\sigma} - i\hbar u_{k\sigma} \\ & \times \sum_{k'} \left[\dot{u}_{k'\sigma} u_{k'\sigma}^* \frac{1}{2\gamma_\sigma^3} (\sin \gamma_\sigma \cos \gamma_\sigma + \gamma_\sigma - 2 \sin \gamma_\sigma) \right. \\ & \left. + \dot{u}_{k'\sigma}^* u_{k'\sigma} \frac{1}{2\gamma_\sigma^2} \left(1 - \frac{\sin \gamma_\sigma \cos \gamma_\sigma}{\gamma_\sigma} \right) \right] = 0 \end{aligned} \quad (3.25)$$

of elimination of the QD-lead tunneling in the transformed Hamiltonian. Here both the tunneling amplitude $V_{k\sigma}$ and transformation parameter $u_{k\sigma}$ are functions of time. Condition (3.25) contains a number of terms with the time derivatives \dot{u}_k . Neglecting these time derivatives would correspond to the adiabatic approximation where the variation in the tunneling amplitude is slow enough and the whole electron system always has enough time to readjust to the varying tunneling amplitude without additional level mixing. Then one can check straightforwardly that Eq. (3.8) with the time-dependent $V_k(t)$ solves Eq. (3.25).

Now we carry out a more general analysis going *beyond* the adiabatic approximation. For this sake we multiply Eq. (3.25) by $u_{k\sigma}^*$ and sum over k , which leads to the equation

$$\begin{aligned} & (\epsilon_d - Z_\sigma) \tan \gamma_\sigma + T_\sigma - T_\sigma^* \tan^2 \gamma_\sigma \\ & = -i\hbar \frac{d}{dt} \tan \gamma_\sigma - i\hbar \frac{\tan \gamma_\sigma}{2\gamma_\sigma^2} \sum_{k'} (\dot{u}_{k'\sigma} u_{k'\sigma}^* - \dot{u}_{k'\sigma}^* u_{k'\sigma}) \end{aligned} \quad (3.26)$$

Substituting Eq. (3.26) into Eq. (3.25) we get the equation

$$\begin{aligned} & u_{k\sigma} [(\epsilon_{k\sigma} - Z_\sigma) \tan \gamma_\sigma + T_\sigma] - \gamma V_{k\sigma} \\ & = -i\hbar \frac{\tan \gamma_\sigma}{\gamma_\sigma^2} u_{k\sigma} \sum_{k'} u_{k'\sigma}^* \dot{u}_{k'\sigma} + i\hbar \dot{u}_{k\sigma} \tan \gamma_\sigma \end{aligned} \quad (3.27)$$

Neglecting the time derivatives of transformation parameter $u_k(t)$ in the r.h.s of Eq. (3.27), which corresponds to the adiabatic approximation, yields Eq. (3.8) with the time-dependent tunneling amplitude $V_k(t)$. All the other equations obtained in Sec. III A also hold. Accounting for the r.h.s. of Eq. (3.27) allows one to obtain nonadiabatic corrections.

Having in mind that the quantities ϵ_d , γ_σ , and Z_σ are explicitly real, we separate real and imaginary parts in Eq. (3.26) and thus get two equations

$$T_\sigma - T_\sigma^* = -2i\hbar \dot{\gamma}_\sigma \quad (3.28)$$

and

$$\begin{aligned}
& (\varepsilon_d - Z_\sigma) \tan \gamma_\sigma + \frac{T_\sigma + T_\sigma^*}{2} (1 - \tan^2 \gamma_\sigma) \\
& = -i\hbar \frac{\tan \gamma_\sigma}{2\gamma_\sigma^2} \sum_{k'} (\dot{u}_{k'\sigma} u_{k'\sigma}^* - \dot{u}_{k'\sigma}^* u_{k'\sigma}). \quad (3.29)
\end{aligned}$$

These equations may be instrumental in looking for solutions $u_{k\sigma}(t)$ for specific problems. It follows from Eq. (3.28) that the quantity T_σ , which was real for the time-independent case, remains real also in the adiabatic approximation for the time-dependent case.

Returning back to the transformed Hamiltonian (3.24), we note that the first term $e^S H e^{-S}$ is now time dependent due to the time dependence of S . Carrying out the transformation in the same fashion, as in the previous section, we get the time-dependent energy level

$$E_{d\sigma} = E_{d\sigma}^{(a)} + E_{d\sigma}^{(b)}, \quad (3.30)$$

where

$$E_{d\sigma}^{(a)} = \frac{\varepsilon_d + Z_\sigma \tan^2 \gamma_\sigma - (T_\sigma + T_\sigma^*) \tan \gamma_\sigma}{1 + \tan^2 \gamma_\sigma} \quad (3.31)$$

is the same energy level (3.12) as before but with the coefficients $Z_\sigma, T_\sigma, T_\sigma^*, \gamma_\sigma$ depending parametrically on time t . Thus, in the adiabatic approximation the time dependence of the resonance level position $E_{d\sigma}^{(a)}(t)$ is determined by Eq. (3.13) with the time-dependent self-energy part

$$L_\sigma(\varepsilon, t) = \sum_k \frac{|V_k(t)|^2}{\varepsilon - \varepsilon_{k\sigma}}. \quad (3.32)$$

There is also the nonadiabatic correction

$$E_{d\sigma}^{(b)}(t) = -\frac{1}{2} i\hbar \frac{\sin^2 \gamma}{\gamma^2} \sum_k (\dot{u}_{k\sigma} u_{k\sigma}^* - \dot{u}_{k\sigma}^* u_{k\sigma}). \quad (3.33)$$

To calculate the coefficients, one has to specify the form of tunneling amplitudes $V_k(t)$. An example of time-dependent tunneling will be considered in the next section.

IV. TUNNEL CONDUCTANCE

In this section we study the tunnel conductance basing on the transformed Hamiltonian \tilde{H} . The tunnel current may be calculated, e.g., by means of the Keldysh technique,³⁰ where the bias eV is included in the zero-order Hamiltonian and the scattering $\sim W_{lk,rk'}$ is considered as a perturbation. First, we calculate the spin-polarized current through an immovable quantum dot and then discuss the modulation of this current due to the oscillatory motion of the dot.

A. Tunneling through static dot

Far from the boundary between the two adjacent charge sectors with $N=1$ and $N=2$, where both levels $\varepsilon_{d\uparrow}^{(1)}$ and $\varepsilon_{d\downarrow}^{(2)}$ are far from the chemical potential μ , the Keldysh method applied to Hamiltonian (3.21) in a single loop approximation gives the conventional golden rule equation

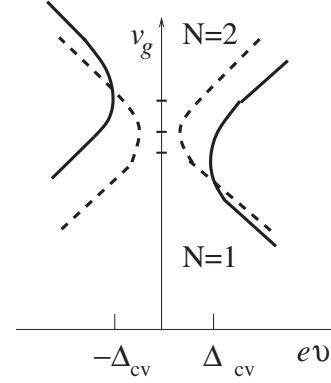


FIG. 3. Coulomb diamonds diagram for tunneling conductance $G(v_g, eV)$ near the border ($N=1$)/($N=2$) for the down-spin and up-spin electrons (solid and dashed lines, respectively). Three bars on the v_g axis mark the values of the gate voltage corresponding to the level $E_{d\downarrow}$ in resonance with ε_c , ε_F , and ε_v (bottom up).

$$\begin{aligned}
I = e \frac{2\pi}{\hbar} \sum_{kk'} \sum_{\sigma} |W_{lk,rk'}^{\sigma}|^2 \delta(\varepsilon_{lk\sigma} + eV - \varepsilon_{rk'\sigma}) \\
\times \{f(\varepsilon_{lk\sigma})[1 - f(\varepsilon_{rk'\sigma})] - f(\varepsilon_{rk'\sigma})[1 - f(\varepsilon_{lk\sigma})]\}, \quad (4.1)
\end{aligned}$$

where eV is the source-drain bias, $f(\varepsilon_{k\sigma})$ is the Fermi distribution function for spin-polarized electrons, and the scattering amplitude $W_{lk,rk'}$ is defined in Eq. (3.16).

The standard Coulomb diamond diagram for tunneling conductance $G(v_g, eV)$ is distorted in the region of gate voltages v_g corresponding to the change in QD occupation ($N=1 \rightarrow N=2$). In the case of completely spin-polarized dots the Coulomb step corresponding to the resonance $E(N=1, v_g) = E(N=2, v_g) - \mu$ in the current-voltage characteristics is absent at zero bias and zero temperature due to the spin blockade. The chemical potential μ is pinned to the Fermi level of spin-up electrons $\varepsilon_{F\uparrow}$, but the resonance level $E_{d\downarrow} = E(N=2) - E(N=1)$ belongs to the down-spin electron (see Fig. 2). Thus the tunneling at zero bias $eV=0$ is suppressed by the spin blockade. This blockade may be surmounted by means of a finite source-drain bias compensating the energy gap. However, the conditions for the onset of spin-up and spin-down tunnel currents are different.

The boundary of the Coulomb diamond with $N=1$ for spin-down electrons follows the evolution of the resonance level $E_{d\downarrow}$ until this level approaches from above the bottom of conduction band $\varepsilon_{c\downarrow}$. When it crosses the band edge, the resonance tunneling is no more possible at $eV < \Delta_{cv}$, so the Coulomb resonance line for $G(v_g, eV)$ deviates from the linear behavior, as it is sketched in Fig. 3 (solid line). Negative-bias part of the Coulomb diamond corresponds to the hole tunneling through the occupied resonance level in the sector $N=2$. It is distorted in the same way in the region of v_g where this level matches the top of the valence band (second branch of the solid line). When the down-spin level is deep enough in the conduction or valence band, the linear behavior is restored again.

The blockade for spin-up electrons near the boundary ($N=1$)/($N=2$) is lifted at eV compensating the spin-flip ex-

citation in the dot. As was mentioned above, the spin-up electron tunneling is allowed provided the dot is excited to the state $E_{d\downarrow}$ given by the solution of Eq. (3.13) for the doubly occupied dot, and the splitting energy may be estimated as $\Delta_{\uparrow\downarrow} \approx |L(E_{d\uparrow}) - L(E_{d\downarrow})|$ (see Ref. 25 for experimental determination of such splitting in the Kondo tunneling regime). The line of resonance tunneling for spin-up electrons is drawn in Fig. 3 by the dashed curve.

Besides, the tunneling transparency is especially sensitive to the position of the dot level in the near vicinity of band edges. The intensity of standard resonance tunneling lines is enhanced for the spin-down electrons in the region of ($ev \approx +\Delta_{cv}, \varepsilon_d - v_g \approx \varepsilon_c$) and ($ev \approx -\Delta_{cv}, \varepsilon_d - v_g \approx \varepsilon_v$). In order to investigate this enhancement, we find the explicit equation for the tunnel conductance from Eqs. (4.1) and (3.16). Transforming summation over kk' by integration over $\epsilon\epsilon'$ in the usual way and performing standard calculations, one gets the equation

$$G_{\downarrow}(v_g, \Delta_{cv}) = \frac{e^2}{h} \frac{\Gamma_l \Gamma_r}{(2\pi^2)} \frac{R^2(\gamma_{\downarrow})}{|E_{d\downarrow} - \varepsilon_c|^2} \left[1 + \frac{R(\gamma_{\downarrow})L(E_{d\downarrow})}{\Delta_{cv}} \right]^2 \quad (4.2)$$

for the threshold value of $ev \rightarrow \Delta_{cv} + o$ in case of 2D electron gas in the planar leads. Here $\Gamma_i = 2\pi V_i^2 S_i$ is the tunneling rate for the lead i obtained in the approximation of $V_{ik} = V_i$ and constant electron density of states $S_i(\varepsilon) = S_i$, which is valid for 2D electrons. It should be taken into account that the definition of the position of resonance level $E_{d\downarrow}$ falling into the conduction-band continuum implies the procedure described below Eq. (3.13). The function $L(\epsilon)$ has a logarithmic singularity at the band edge, $\text{Re } L(\epsilon \rightarrow \varepsilon_c) \sim -\ln(|\epsilon - \varepsilon_c|/\Delta_{cv})$. As a result, Eq. (3.13) has either one or two solutions depending on a position of the level $\varepsilon_{d\downarrow}^{(2)} - v_g$ relative to the band edge.³¹

The resonance factor $|E_{d\downarrow} - \varepsilon_c|^2$ in the denominator and the singular factor $L(E_{d\downarrow})$ in the numerator of Eq. (4.2) result in a noticeable enhancement of G at the boundary of Coulomb diamond. This enhancement is characterized by the evolution of the ratio

$$\rho(v_g) = \frac{R^2(\gamma_{\downarrow})}{|E_{d\downarrow} - \varepsilon_c|^2} \quad (4.3)$$

from its value in the middle of Coulomb diamond to that in the vicinity the point $\varepsilon_d(v_g) = \varepsilon_c$. Here and below we omit the superscript (2) in the notation of ε_d . Far from the Coulomb resonance the difference between $|E_{d\downarrow}|$ and ε_d is small and $\tan^2 \gamma_{\downarrow} \sim V^2/(\varepsilon_d - \varepsilon_c)^2 \ll 1$. The function $R(\gamma_{\downarrow})$ tends to 1/2 in this limit, so that the factor ρ may be estimated as $\rho \approx 1/4(\varepsilon_d - \varepsilon_c)^2$. Near the band edge ε_c the factor $R(\gamma_{\downarrow}) \approx \cot \gamma_{\downarrow} = \sqrt{|E_{d\downarrow} - \varepsilon_c|/\Gamma_r}$ [see Eqs. (3.9) and (3.17)], so that $\rho \sim [|E_{d\downarrow} - \varepsilon_c|/\Gamma_r]^{-1}$. Numerical estimates of this enhancement are presented at Fig. 4. In these calculations the density of states was assumed to be constant in the lower part of 2D conduction band, so that the self-energy in the r.h.s. of Eq. (3.13) may be approximated as $L(E) \approx \Gamma_r \ln(E/D)$, where D is the effective width of conduction band and the argument E is complex. Then the solutions $E = E_{d\downarrow}$ of Eq. (3.13) are expressed via the Lambert W function $W(n, x)$,

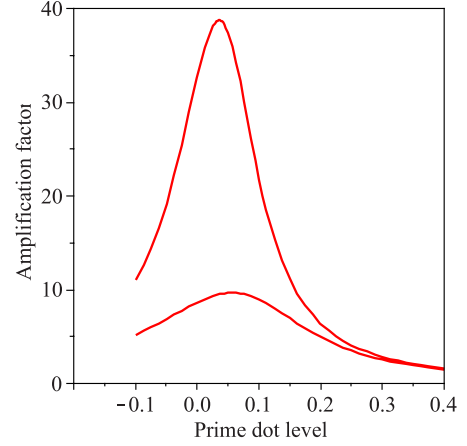


FIG. 4. (Color online) Amplification factor $\rho(\varepsilon_d^{(2)})$ for two values of tunneling rate $\Gamma/D=0.01$ (lower curve) and $\Gamma/D=0.02$ (upper curve) as a function of the prime dot level position $\varepsilon_d(v_g)$. The evolution of the resonance level $E_{d\downarrow}$ is given by Eq. (4.4) with $n=1$. This resonance approaches the conduction-band edge with $\varepsilon_d \rightarrow +0$ and the amplification factor (4.3) achieves its maximal value under these conditions.

$$E_{d\downarrow} = -\Gamma_r W(n, -\Gamma_r^{-1} e^{-\varepsilon_d/\Gamma_r}) \quad (4.4)$$

(here the reference point is $\varepsilon_c=0$, all energy parameters are measured in units D , and index n enumerates branches of the W function). There are two solutions for $E_{d\downarrow}$ near the band edge.³¹ The principal branch $n=0$ gives the discrete level in the gap, and the branch $n=1$ corresponds to the resonance in the band, which is of interest for us here.

Thus the magnitude of conductance peak on the resonance lines of Coulomb diamond diagram for spin-down electrons (Fig. 3) as a function of the gate voltage v_g should follow the curves plotted in Fig. 4. The amplification reaches its maximum when the difference $|E_{d\downarrow} - \varepsilon_c|$ comes up to Γ_r ; therefore, the smaller the Γ_r , the stronger the enhancement factor ρ . The factor $R(\gamma_{\downarrow})L(E_{d\downarrow})/\Delta_{cv}$ in the square brackets in Eq. (4.2) behaves as $\epsilon^{1/2} \ln \epsilon$ in the vicinity $\epsilon = |E_{d\downarrow} - \varepsilon_c|$ of the band edge and thus gives additional contribution to this enhancement. Both analytical and numerical estimates confirm this statement. Experimentally, this effect should be observed as an increase in the tunneling conductance on the boundary of Coulomb diamond in the vicinity of the threshold value of $ev_{th} = \Delta_{cv}$. A similar effect should arise on the hole side of the Coulomb diamond diagram ($ev_{th} = -\Delta_{cv}$), when the occupied level $E_{d\downarrow}$ crosses the top of the down-spin valence band (solid lines in Fig. 3).

To conclude the dependence of tunneling conductance on ev and v_g near the occupation border ($N=1$)/($N=2$) radically differs from that for the standard Coulomb diamond diagram. (i) The Coulomb step $G(v_g)$ is absent at $|ev| \rightarrow 0$. (ii) The diamond boundaries are split due to the spin polarization of carriers. The spin-up boundary is symmetric relative to the change in the bias sign, and the threshold value for $G_{\uparrow}(ev)$ at v_g corresponding to a Coulomb resonance for the spin-up electrons is given by the induced molecular field for dot electrons $ev_{th} = E_{d\downarrow} - E_{d\uparrow}$ (3.13). The threshold value for $G_{\downarrow}(ev)$ is $ev_{th} = \Delta_{cv}$ and the spin-down resonance lines are

shifted downward relative to G_{\uparrow} for the left-right tunneling (positive bias) and upward for right-left tunneling (negative bias). (iii) The amplitude of the Coulomb resonance line $G_{\downarrow}(v_g, e\nu)$ in the vicinity of $e\nu_{th}$ should follow the profile shown in Fig. 4.

B. Tunneling through moving dot

As is shown above, the canonical transformation allows one to distinguish between the adiabatic and nonadiabatic contributions to the tunneling amplitude. Let us first discuss the adiabatic corrections to the inelastic current given by Eq. (4.1) and illustrated by Fig. 4. In the vicinity of the point $(N=1)/(N=2)$ of the Coulomb diamond diagram, the adiabatic position of the down-spin level $E_{d\downarrow}^{(a)}$ given by the solution of the equation

$$E_{d\downarrow}^{(a)}(t) = \sum_k \frac{|V_{jk}(t)|^2}{E_{d\downarrow}^{(a)}(t) - \epsilon_k} \quad (4.5)$$

rocks around ϵ_{cr} or ϵ_{vl} (see Fig. 2). This solution depends parametrically on time via the oscillating tunnel coupling $|V_{jk}(t)|^2$. The above analysis of the static case prompts that time-dependent corrections become significant at a finite bias close to the threshold value $e\nu_{th} = \pm \Delta_{cv}$. The adiabatic evolution of the level $E_{d\downarrow}^{(a)}$ in time near ϵ_c is given by the same equation (4.4), where the tunneling rate Γ_r parametrically depends on t . If the time-dependent perturbation is weak in comparison with the static value of tunneling rate, the temporal component of $E_{d\downarrow}^{(a)}$ may be found perturbatively. Representing the tunneling rate as $\Gamma_r = \Gamma_{r0} + \delta\Gamma(t)$ and expanding Eq. (4.4) around the time-independent value marked by index “0,” we get

$$E_{d\downarrow}^{(a)}(t) = E_{d\downarrow}^{(0)} - \frac{W_0}{1 + W_0} \left(\frac{\epsilon_d}{\Gamma_{r0}} + W_0 \right) \delta\Gamma(t). \quad (4.6)$$

When deriving Eq. (4.6), the equality $W(x) = x[1 + W(x)]dW/dx$ is used.

This time dependence turns into the corresponding adiabatic time dependence of tunnel conductance, mainly via the enhancement factor $\rho(E_{d\downarrow})$ (4.3). One may expect that the slow adiabatic variations in $G(t)$ will be especially distinct at v_g corresponding to steep slopes of $\rho(t)$ (Fig. 4) at $e\nu \sim \pm \Delta_{cv}$ near the boundary $(N=1)/(N=2)$ of the Coulomb diamond diagram (Fig. 3).

C. Weak time-dependent perturbation

Calculation accounting for nonadiabatic corrections to tunnel conductance is generally an extremely complicated nonlinear problem. To make it tractable, we assume that the time-dependent part of $V_{jk\sigma}$ is only a small periodic perturbation with respect to the time-independent part $V_{jk\sigma}^{(0)}$ and consider only the linear response given by the first harmonics. The nonlinear effects will be discussed separately. This approach allows one to pick up first nonadiabatic corrections to tunneling amplitude $W_{kk'}$, which turns out to be small everywhere except in the vicinity of band edges.

Let us assume that the tunneling integral has the form

$$V_k(t) = V_k^{(0)} + V_k^{(1)} \cos \omega t \quad (4.7)$$

(here and below indices $j\sigma$ are omitted for the sake of brevity). Here $V_k^{(0)} \gg V_k^{(1)}$. The solution of Eq. (3.25) is looked for in the form

$$u_k = u_k^{(0)} + u_k^{(1)} \cos \omega t + i v_k^{(1)} \sin \omega t, \quad (4.8)$$

where the time-dependent corrections to $u_k^{(0)}$ are also small. Then we vary all the coefficients in Eq. (3.28) with respect to $u_k^{(0)} = g_k V_k^{(0)}$ [see Eq. (3.8)] and $V_k^{(0)}$ and collect separately all the terms containing $\cos \omega t$ and $\sin \omega t$, respectively. Substituting then u_k in Eq. (3.15), we reduce the scattering amplitude $W_{kk'}$ to the following form:

$$W_{kk'} = \bar{W}_{kk'} + W_{kk'}^{(1)} \cos \omega t + \hbar \omega W_{kk'}^{(2)} \sin \omega t, \quad (4.9)$$

where the coefficients of the cosine and sine terms can be explicitly calculated. The cosine coefficient

$$W_{kk'}^{(1)} = \sum_q \left[\frac{\delta \bar{W}_{kk'}}{\delta V_q} V_q^{(1)} + \frac{\delta \bar{W}_{kk'}}{\delta V_q^*} V_q^{(1)*} \right] \quad (4.10)$$

is obtained by varying Eq. (3.16) over the hybridization potential V_q , whereas the sine coefficient

$$W_{kk'}^{(2)} = i \sum_q g_q^2 \left[\frac{\delta W_{kk'}}{\delta u_q} V_q^{(1)} - \frac{\delta W_{kk'}}{\delta u_q^*} V_q^{(1)*} \right] + W_{kk'}^{(2), nonad} \quad (4.11)$$

is obtained by varying the more general equation (3.15) over the transformation parameter u_q . After the variation, u_k in the form Eq. (3.8) can be substituted. Then

$$W_{kk'}^{(2), nonad} = -i \left[\frac{V_{k'}^{(1)*} V_k^{(0)} - V_k^{(1)} V_{k'}^{(0)*}}{\Delta_{k\sigma} \Delta_{k'\sigma}} \tilde{R}(\gamma_\sigma) + \frac{V_k^{(0)} V_{k'}^{(0)*}}{2 \Delta_{k\sigma} \Delta_{k'\sigma}} \tilde{R}^2(\gamma_\sigma) \sum_{k''} \frac{V_{k''}^{(1)} V_{k''}^{(0)*} - V_{k''}^{(0)*} V_{k''}^{(1)}}{\Delta_{k''\sigma} \Delta_{k'\sigma}} \right]$$

with

$$\tilde{R}_\sigma = \frac{R_\sigma}{\sqrt{1 + \tan^2 \gamma_\sigma}}.$$

The most divergent terms in Eqs. (4.10) and (4.11) appear when we vary only explicitly written $V_k^{(0)}$ in Eq. (3.16) and $u_{k'}$ in Eq. (3.15). As a result keeping only these most divergent terms we have

$$W_{kk'}^{(1)} = (V_k^{(0)} V_{k'}^{(1)*} + V_{k'}^{(0)*} V_k^{(1)}) K^\sigma \left(\frac{1}{\Delta_{k\sigma}} + \frac{1}{\Delta_{k'\sigma}} \right) R(\gamma_\sigma) \quad (4.12)$$

and

$$W_{kk'}^{(2)} = -i (V_k^{(0)} V_{k'}^{(1)*} - V_{k'}^{(0)*} V_k^{(1)}) K^\sigma \left(\frac{1}{\Delta_{k\sigma}^2} + \frac{1}{\Delta_{k'\sigma}^2} \right) R(\gamma_\sigma) \frac{\gamma_\sigma}{\tan \gamma_\sigma}. \quad (4.13)$$

The corresponding corrections to the tunneling transparency near the conductance band edge behave as

$$\delta G_{\downarrow}^{(1)}(v_g, \Delta_{cv}) \approx \frac{e^2 \Gamma_r \Gamma_r^{(1)}}{h (2\pi^2)} \frac{R^2(\gamma_{\downarrow})}{|E_{d\downarrow} - \varepsilon_c|^2} \cos \omega t \quad (4.14)$$

and

$$\delta G_{\downarrow}^{(2)}(v_g, \Delta_{cv}) \approx (\hbar \omega) \frac{e^2 \Gamma_r \Gamma_r^{(2)}}{h (2\pi^2)} \frac{R^2(\gamma_{\downarrow})}{|E_{d\downarrow} - \varepsilon_c|^{5/2}} \frac{\pi}{2\sqrt{\Gamma_r}} \sin \omega t, \quad (4.15)$$

where

$$\Gamma_r^{(m)} = 2\pi S_r [i^{(m-1)} V_r^{(1)} V_r^{(0)*} + (-i)^{(m-1)} V_r^{(0)} V_r^{(1)*}]$$

is the adiabatic correction to the tunneling rate for $m=1$ and the correction due to weak nonadiabatic effect for $m=2$. Equation (4.15) uses the fact that

$$\gamma_{\downarrow} \rightarrow \frac{\pi}{2}, \quad \tan \gamma_{\downarrow} = \sqrt{-\frac{dL}{d\varepsilon}} \approx \sqrt{\frac{\Gamma_r}{|E_{d\downarrow} - \varepsilon_c|}}$$

for $E_{d\downarrow} \rightarrow \varepsilon_c$ when $|E_{d\downarrow} - \varepsilon_c| \approx \Gamma_r$. We use here the approximation $V_{k'}^{(m)} \approx V_r^{(m)}$ similarly to the one used in Eq. (4.2).

The term with the sine in Eq. (4.9) causes a phase shift between the oscillations of the hybridization parameter and the resulting current through the dot. If we neglect the k dependence of coefficients (4.10) and (4.11), this phase shift can be readily found:

$$\varphi = -\arctan\left(\frac{\delta G_{\downarrow}^{(2)}(v_g, \Delta_{cv})}{\delta G_{\downarrow}^{(1)}(v_g, \Delta_{cv})}\right).$$

It is expected to be generally rather small due to the factor $g_k \hbar \omega$, which is usually very small unless the dot level approaches the band edge ε_c . Close to the edge this factor diverges and results in an increasing phase shift,

$$\varphi \approx -\arctan \frac{\hbar \omega \Gamma_r^{(2)}}{\Gamma_r^{(1)} \sqrt{\Gamma_r} |E_{d\downarrow} - \varepsilon_c|} \approx -\arctan \frac{\hbar \omega \Gamma_r^{(2)}}{\Gamma_r \Gamma_r^{(1)}}.$$

As a result the phase shift φ may become essential at $E_{d\downarrow} \rightarrow \varepsilon_c$.

The nonadiabatic corrections to tunneling conductance acquire the simple form of phase shift in oscillating cosine function only as long as the parameter $f_k = g_k \hbar \omega \sim \hbar \omega / \Delta$ is small and the perturbative approach is valid. With increasing f_k one may expect appearance of higher harmonics $n\omega$ in oscillating conductance. With an increase in the amplitude $V^{(1)}$ the language of quasienergy levels³² is more appropriate. We plan to discuss this approach elsewhere.

V. CONCLUDING REMARKS

We have displayed in this paper an approach to the Anderson model for a half-metallic electron liquid in a tunnel contact with a moving nanoshuttle under strong Coulomb blockade. It is shown that in the situation where the spin-flip cotunneling processes are suppressed at low energies, the exact canonical transformation eliminating the tunneling

term in the Anderson Hamiltonian exists even in the presence of strong Hubbard repulsion in the shuttle and time-dependent lead-shuttle tunneling. This canonical transformation in principle allows one to sort out the slow adiabatic renormalization of the energy levels and the tunnel transparency and to consider nonadiabatic corrections at least perturbatively. One may also include the inelastic spin-flip processes in the canonical transformation in the fourth order of perturbation theory in V_i , but these weak corrections do not change the above qualitative picture. We also have calculated the weak nonadiabatic corrections to tunneling transparency in a specific model of periodic sinusoidal motion of the shuttle. Undoubtedly, strong nonadiabatic effects should be taken into account in a more refined scheme: in the case of a periodic time-dependent perturbation one should appeal to the Floquet theorem in the time domain and use the quasienergy language.^{32,33}

Because of the energy gap for spin-flip processes in the half-metallic leads the Kondo cotunneling processes are suppressed, and the zero-bias anomaly in the tunnel conductance is absent. Physical manifestations of the shuttling mechanism under discussion arise in the form of time-dependent enhancement of conductance at finite bias near the boundaries of Coulomb diamonds on the phase diagram $G(v_g, eV)$. The boundaries themselves are distorted due to the complete spin polarization of carriers (see Fig. 3), and even the Coulomb blockade step corresponding to occupation change from odd to even number of electrons in the dot is absent at zero bias. One may expect appearance of quasienergy satellites in this part of the phase diagram $G(v_g, eV)$ when the shuttle motion is essentially nonadiabatic. This regime is a subject for future studies.

Experimental investigation of shuttling in a single electron tunneling regime is a rapidly developing field. Recent progress in revealing the features of Coulomb blockade in mechanical single electron transistors^{13,34} supports our hope that the studies of adiabatic and nonadiabatic shuttling will obtain firm experimental substantiation in a near future.

APPENDIX A: TIME-DEPENDENT CANONICAL TRANSFORMATION

To diagonalize the Schrödinger equation (3.23) for the wave function $\tilde{\psi} = e^{S(t)} \psi$, we conjecture the form

$$\tilde{H} = e^S H e^{-S} + S_1$$

for the canonically transformed Hamiltonian. Then substituting \tilde{H} and $\tilde{\psi}$ into Eq. (3.23), we obtain

$$i\hbar \left(\frac{\partial}{\partial t} e^S \right) \psi + i\hbar e^S \frac{\partial \psi}{\partial t} = (e^S H e^{-S} + S_1) e^S \psi. \quad (A1)$$

The time derivative of exponent is found by means of the operator equation

$$\frac{d}{dt} e^S = \int_0^1 e^{\lambda S} \dot{S} e^{-\lambda(S-1)} d\lambda = e^S \left[\int_0^1 e^{-\lambda S} \dot{S} e^{\lambda S} d\lambda \right]. \quad (A2)$$

Then using Eqs. (A2) and (3.22) in Eq. (A1) yields

$$i\hbar \left[\int_{\lambda=0}^1 d\lambda e^{\lambda S} \dot{S} e^{-\lambda S} \right] e^S \psi + e^S H \psi = e^S H \psi + S_1 e^S \psi.$$

from where we straightforwardly get S_1 and Eq. (3.24).

APPENDIX B: TUNNELING AMPLITUDE FOR WEAK PERIODIC POTENTIAL

To derive the first nonvanishing time-dependent corrections to the tunneling procedure, we vary the terms in Eq. (3.28). This variation procedure results in the two linear equations

$$\begin{aligned} u_k^{(1)*} V_k^{(0)} - u_k^{(1)} V_k^{(0)*} - \hbar \omega g_k (V_k^{(0)*} v_k^{(1)} - v_k^{(1)*} V_k^{(0)}) \\ = -g_k (V_k^{(0)*} V_k^{(1)} - V_k^{(0)} V_k^{(1)*}), \\ v_k^{(1)*} V_k^{(0)} + V_k^{(0)*} v_k^{(1)} + \hbar \omega g_k (V_k^{(0)*} u_k^{(1)} + u_k^{(1)*} V_k^{(0)}) = 0, \end{aligned} \quad (\text{B1})$$

where g_k is explicitly real as defined in Eq. (3.8). Spin index σ is suppressed.

The first of these equations contains only explicitly imaginary terms whereas the second one contains only real terms. Therefore we have only two equation for four real variables (two complex variables). It is readily verified that

$$\begin{aligned} \bar{u}_k^{(1)} &= \frac{g_k}{1 - (\hbar \omega g_k)^2} V_k^{(1)}, \\ \bar{v}_k^{(1)} &= -\frac{\hbar \omega g_k^2}{1 - (\hbar \omega g_k)^2} V_k^{(1)} \end{aligned} \quad (\text{B2})$$

is a particular solution of the set of equations (B1). One can also see that in the limit $g_k \hbar \omega \rightarrow 0$ this solution reduces to the adiabatic approximation where we can take the results obtained in Sec. III A for the time-independent problem and substitute there the tunneling amplitude (4.7) slowly varying in time.

The general solution of the corresponding homogenous set of equations reads

$$\begin{aligned} u_k^{(1)} &= -\frac{1}{2} \left(\hbar \omega g_k + \frac{1}{\hbar \omega g_k} \right) (C_{1k} + i C_{2k}) \\ &\quad + \left(\hbar \omega g_k - \frac{1}{\hbar \omega g_k} \right) \frac{V_k^{(0)}}{2 V_k^{(0)*}} (C_{1k} - i C_{2k}), \\ \bar{v}_k^{(1)} &= C_{1k} + i C_{2k}. \end{aligned} \quad (\text{B3})$$

It should be added to the particular solution (B2). The parameters C_{1k} and C_{2k} are meanwhile arbitrary. These parameters determined from the original cancellations (3.25)–(3.29) turn out to be small, $C_1, C_2 \sim (g_k \hbar \omega)^3$, and may result at most in nonadiabatic corrections $\sim (g_k \hbar \omega)^2$.

In order to calculate the tunnel current we need the scattering matrix element

$$W_{kk'} = W_{kk'}^{ad} + W_{kk'}^{nonad}, \quad (\text{B4})$$

where the first term $W_{kk'}^{ad}$ is obtained by substituting solutions (4.8) and (B2) into Eq. (3.15) and keeping the terms linear in $g_k \hbar \omega$. This contribution remains finite in the adiabatic limit $g_k \hbar \omega \rightarrow 0$. However it contains also nonadiabatic corrections due to the third term in Eq. (4.8). These corrections are determined by the equation

$$\begin{aligned} W_{kk'}^{nonad} &= i\hbar (\dot{u}_k^* u_{k'} - \dot{u}_k u_{k'}^*) \frac{1 - \cos \gamma}{\gamma^2} \\ &\quad + i\hbar u_k u_{k'}^* \frac{(\cos \gamma - 1)^2}{2\gamma^4} \sum_{k''} (\dot{u}_{k''} u_{k''}^* - \dot{u}_{k''}^* u_{k''}), \end{aligned} \quad (\text{B5})$$

which contains derivatives \dot{u}_k and, hence, is purely nonadiabatic, i.e., it disappears in the limit $g_k \hbar \omega \rightarrow 0$. Keeping only terms linear in $g_k \hbar \omega$ in the scattering matrix element (B4), we come to Eq. (4.9).

¹L. I. Glazman and M. Pustilnik, in *Nanophysics: Coherence and Transport*, edited by H. Bouchiat, Y. Gefen, S. Gueron, G. Montambaux, and J. Dalibard (Elsevier, New York, 2005), p. 427.

²R. Hanson, L. P. Kouwenhoven, J. R. Petta, S. Tarucha, and L. M. K. Vandersypen, *Rev. Mod. Phys.* **79**, 1217 (2007).

³H. Park, J. Park, A. Lim, E. Anderson, A. Alevisatos, and P. McEuen, *Nature (London)* **407**, 57 (2000).

⁴L. H. Yu and D. Natelson, *Nano Lett.* **4**, 79 (2004).

⁵N. Roch, S. Florens, V. Bouchiat, W. Wernsdorfer, and F. Balestro, *Nature (London)* **453**, 633 (2008).

⁶M. Bode, O. Pietzsch, A. Kubetzka, and R. Wiesendanger, *Phys. Rev. Lett.* **92**, 067201 (2004).

⁷C. F. Hirjibehedin, C.-Y. Lin, A. F. Otte, M. Ternes, C. P. Lutz, B. A. Jones, and A. J. Heinrich, *Science* **317**, 1199 (2007).

⁸Y. Goldin and Y. Avishai, *Phys. Rev. Lett.* **81**, 5394 (1998).

⁹A. Kaminski, Yu. V. Nazarov, and L. I. Glazman, *Phys. Rev. B* **62**, 8154 (2000).

¹⁰M. N. Kiselev, K. Kikoin, Y. Avishai, and J. Richert, *Phys. Rev. B* **74**, 115306 (2006).

¹¹L. Y. Gorelik, A. Isacsson, M. V. Voinova, B. Kasemo, R. I. Shekhter, and M. Jonson, *Phys. Rev. Lett.* **80**, 4526 (1998).

¹²D. V. Scheible and R. H. Blick, *Appl. Phys. Lett.* **84**, 4632 (2004).

¹³D. R. Koenig, E. M. Weig, and J. P. Kotthaus, *Nat. Nanotechnol.* **3**, 482 (2008).

¹⁴K. A. Al-Hassanieh, C. A. Busser, G. B. Martins, and E. Dagotto, *Phys. Rev. Lett.* **95**, 256807 (2005).

¹⁵L. I. Glazman and M. E. Raikh, *Pis'ma Zh. Eksp. Teor. Fiz.* **47**, 378 (1988) [*JETP Lett.* **47**, 452 (1988)].

¹⁶T. K. Ng and P. A. Lee, *Phys. Rev. Lett.* **61**, 1768 (1988).

¹⁷M. N. Kiselev, K. Kikoin, R. I. Shekhter, and V. M. Vinokur, *Phys. Rev. B* **74**, 233403 (2006).

- ¹⁸A. Goker, Solid State Commun. **148**, 230 (2008).
- ¹⁹R. López, R. Aguado, and G. Platero, Phys. Rev. Lett. **89**, 136802 (2002).
- ²⁰J. Martinek, Y. Utsumi, H. Imamura, J. Barnaś, S. Maekawa, J. König, and G. Schön, Phys. Rev. Lett. **91**, 127203 (2003).
- ²¹B. R. Buřka and S. Lipiński, Phys. Rev. B **67**, 024404 (2003).
- ²²M.-S. Choi, D. Sanchez, and R. Lopez, Phys. Rev. Lett. **92**, 056601 (2004).
- ²³Y. Tanaka and N. Kawakami, J. Phys. Soc. Jpn. **73**, 2795 (2004).
- ²⁴Y. Qi, J.-X. Zhu, S. Zhang, and C. S. Ting, Phys. Rev. B **78**, 045305 (2008).
- ²⁵A. N. Pasupathy, R. C. Bialczak, J. Martinek, J. E. Grose, L. A. K. Donev, P. L. McEuen, and D. C. Ralph, Science **306**, 86 (2004).
- ²⁶M. I. Katsnelson, V. Yu. Irkhin, L. Chioncel, A. I. Lichtenstein, and R. A. de Groot, Rev. Mod. Phys. **80**, 315 (2008).
- ²⁷T. Jungwirth, J. Sinova, J. Masek, J. Kucera, and A. H. MacDonald, Rev. Mod. Phys. **78**, 809 (2006).
- ²⁸K. A. Kikoin and V. N. Fleurov, Zh. Eksp. Teor. Fiz. **77**, 1062 (1979) [Sov. Phys. JETP **50**, 535 (1979)].
- ²⁹K. A. Kikoin and V. N. Fleurov, *Transition Metal Impurities in Semiconductors* (World Scientific, Singapore, 1994).
- ³⁰L. V. Keldysh, Zh. Eksp. Teor. Fiz. **47**, 1515 (1962) [Sov. Phys. JETP **20**, 1018 (1965)].
- ³¹F. D. M. Haldane and P. W. Anderson, Phys. Rev. B **13**, 2553 (1976).
- ³²Y. B. Zel'dovich, Sov. Phys. Usp. **16**, 427 (1973).
- ³³S. R. Barone, M. A. Narowich, and F. J. Narowich, Phys. Rev. A **15**, 1109 (1977).
- ³⁴D. Koenig, Ph.D. thesis, Ludwig-Maximilians-Universität, München, 2008.